Molecular Cancer Research

Ezrin Promotes Stem Cell Properties in Pancreatic Ductal Adenocarcinoma

Vesselin R. Penchev[1], Yu-Tai Chang[1], Asma Begum[1], Theodore Ewachiw[1], Christian Gocke[1], Joey Li[1], Ross H. McMillan[1], Qiuju Wang[1], Robert Anders[2], Luigi Marchionni[1], Anirban Maitra[3], Aykut Uren[4], Zeshaan Rasheed[1], and William Matsui[1,2]

Abstract

Self-renewal maintains the long-term clonogenic growth that is required for cancer relapse and progression, but the cellular processes regulating this property are not fully understood. In many diseases, self-renewal is enhanced in cancer stem cells (CSC), and in pancreatic ductal adenocarcinoma (PDAC), CSCs are characterized by the surface expression of CD44. In addition to cell adhesion, CD44 impacts cell shape and morphology by modulating the actin cytoskeleton via Ezrin, a member of the Ezrin/Radixin/Moesin (ERM) family of linker proteins. We examined the expression of Ezrin in PDAC cells and found higher levels of both total and activated Ezrin in CSCs compared with bulk tumor cells. We also found that the knockdown of Ezrin in PDAC cells decreased clonogenic growth, self-renewal, cell migration, and CSC frequency *in vitro* as well as tumor initiation *in vivo*. These effects were associated with cytoskeletal changes that are similar to those occurring during the differentiation of normal stem cells, and the inhibition of actin remodeling reversed the impact of Ezrin loss. Finally, targeting Ezrin using a small-molecule inhibitor limited the self-renewal of clinically derived low-passage PDAC xenografts. Our findings demonstrate that Ezrin modulates CSCs properties and may represent a novel target for the treatment of PDAC.

Implications: Our findings demonstrate that Ezrin modulates CSCs' properties and may represent a novel target for the treatment of PDAC.

Introduction

Cancer stem cells (CSC) have been identified in many cancers based on their enhanced tumor-initiating and self-renewal potential that implicates an important role in long-term disease maintenance, progression, and relapse (1, 2). Multiple groups have identified CSCs in pancreatic ductal adenocarcinoma (PDAC) that are enriched in migration, invasion, and drug resistance in addition to clonogenic growth and self-renewal (3–5). Importantly, CSCs appear to be clinically relevant as their presence in primary tumors is associated with the development of metastatic disease and shorter overall survival (OS; ref. 5). Thus, novel strategies targeting CSCs may improve outcomes in PDAC.

In many solid tumors, including PDAC, CSCs express CD44 and HGFR/c-Met, and the expression of these antigens are associated with poor survival (3, 6–8). Several signaling events occur downstream of CD44, including cytoskeletal remodeling that involves Ezrin, a member of the Ezrin/Radixin/Moesin (ERM) family of membrane-cytoskeletal linker proteins that bridges the cytoplasmic tail of CD44 with F-actin (9–14). Ezrin expression is associated with decreased OS and the development of distant metastases in osteosarcoma, soft-tissue sarcomas, as well as colorectal, breast, and hepatocellular carcinomas (15–19). In PDAC, Ezrin activation is associated with shorter OS (20, 21) and impacts the growth and motility of PDAC cell lines (22, 23). Despite these findings, the role of Ezrin in PDAC CSC biology is unknown.

We found that PDAC CSCs express higher levels of Ezrin relative to bulk tumor cells. The inhibition of Ezrin using knockdown studies or a small-molecule antagonist decreased CSC frequency, tumor-initiating potential, and self-renewal. In addition, the effects of Ezrin loss were inhibited by blocking actin polymerization. These results demonstrate that Ezrin impacts stem cell properties in PDAC and may represent a novel target in this disease.

Materials and Methods

Cell culture

MIA PaCa-2 cells were obtained from the ATCC and authenticated by short tandem repeat profiling at the Johns Hopkins Genetics Core Resources Facility. L3.6pl cells were a kind gift of J. Fidler (24). E3LZ 10.7 cells have been described previously as

[1]Department of Oncology, Sydney Kimmel Comprehensive Cancer Center, Johns Hopkins University School of Medicine, Baltimore, Maryland. [2]Department of Pathology, Johns Hopkins University School of Medicine, Baltimore, Maryland. [3]Department of Pathology, University of Texas M.D. Anderson Cancer Center, Houston, Texas. [4]Department of Oncology, Lombardy Comprehensive Cancer Center, Georgetown University Medical Center, Washington, D.C.

Note: Supplementary data for this article are available at Molecular Cancer Research Online (http://mcr.aacrjournals.org/).

Current address for W. Matsui: LIVESTRONG Cancer Institutes, Dell Medical School, University of Texas at Austin, Austin, Texas.

Corresponding Author: William Matsui, Dell Medical School, University of Texas, Austin, Health Discovery Building, 1701 Trinity Street, Mailstop Z1100, Austin, TX 78704. Phone: 512-495-5509; Fax: 512-495-5480; E-mail: william.matsui@austin.utexas.edu

doi: 10.1158/1541-7786.MCR-18-0367

Pa03C (25). All cell lines were cultured in complete media consisting of high-glucose DMEM (Invitrogen) supplemented with 10% FBS (Sigma-Aldrich), 1% penicillin–streptomycin (Invitrogen), and1% L-glutamine (Invitrogen). Cells were treated with NSC305787 (NCI Developmental Therapeutics Program, Bethesda, MD), Cytochalasin D (Tocris Bioscience), or Y-27632 (Sigma-Aldrich) for 72 hours. Tumor colony formation in methylcellulose was carried out as described previously (5).

Ezrin knockdown and overexpression

Short hairpin RNA (shRNA) oligonucleotides were synthesized based on siRNA sequences against Ezrin (GE Dharmacon, siRNA1 catalog no: D-017370-05-0002, siRNA2 cat. #: D-017370-06-0002) or firefly luciferase (ref – FAK paper?) and cloned into the Tet-pLKO-puro lentiviral vector (Addgene). Following transduction, cells were selected with puromycin (2 μg/mL, Thermo Fisher Scientific). For overexpression studies, cDNA encoding the Ezrin-mutant T567D that contains a threonine to aspartic acid substitution at residue 567 (kindly provided by Dr. Chand Khanna, NIH, Bethesda, MD) was cloned into the pInducer20 lentiviral vector using the Gateway Cloning System (Thermo Fisher Scientific; ref. 26). A self-ligated empty pInducer20 construct was used as a control. Cell lines were transduced, and stable lines were selected using G418 sulfate (1.2 mg/mL, Corning).

Animal care, low-passage–derived patient xenografts, and tumor sphere formation

All animal experiments were approved by the Johns Hopkins University Animal Care and Use Committee. Low-passage xenografts were generated from primary surgical specimens collected at the Johns Hopkins Hospital (Baltimore, MD), serially passaged in nude mice, and prepared as single-cell suspensions as described previously (5, 27). Tumor spheres enriched in CSCs were generated by culturing cells (2×10^5 cells/mL) in 60-mm ultralow attachment plates (Corning) and DMEM/F-12 (1/1) media (Invitrogen) supplemented with 1X B-27 supplement (Thermo Fisher Scientific), 20 ng/mL bFGF (Invitrogen), 1% penicillin–streptomycin, and 1% L-glutamine. Tumor cell differentiation was induced by culturing cells in complete media containing 10% FBS.

Tumor-initiating cell (TIC) frequency was determined by injecting L3.6pl cells (1×10^5) in serum-free DMEM and Matrigel (BD Biosciences) subcutaneously into the flanks of NSG mice. Following tumor formation, mice were provided doxycycline (2 mg/mL, Sigma-Aldrich) in 5% sucrose. After 9 days of treatment, tumors were collected, dissociated, and depleted of mouse cells then injected (50, 100, 250, and 500 cells) into secondary recipients. Tumor formation was monitored for 30 days, and (TIC) frequency was calculated using extreme limiting dilution analysis (ELDA; ref. 28).

Flow cytometry

Cells were stained for surface antigen expression with anti–CD44-APC (BD Biosciences), anti–CD24-PE/FITC (BD Biosciences), anti–c-Met-PE (R&D Systems), and anti–CD133-APC (Miltenyi Biotec). Cells were analyzed using a BD FACSCalibur (BD Biosciences) flow cytometer to identify CSC populations (8, 29, 30). Intracellular staining was carried out using the Cytofix/Cytoperm Kit (BD Biosciences) and anti-Ezrin (Cell Signaling Technology) or anti-pERM (Cell Signaling Technology) antibodies, goat anti-rabbit-AlexaFluor488 (Invitrogen), phalloidin-TRITC/FITC (Sigma-Aldrich), or DNAse1-AlexaFluor488 (Sigma-Aldrich).

qRT-PCR

Total mRNA was extracted and depleted of genomic DNA using the RNeasy PlusMini Kit (Qiagen) and reverse-transcribed with SuperScript III reverse transcriptase (Invitrogen). qRT-PCR was performed using Taqman Probes (GAPDH probe #: hs099999905, Ezrin probe #:hs00931653; Applied Biosystems).

Cell migration assay

Cells were cultured in 24-well inserts with 8-μm pores (BD Biosciences) for 24 hours. Cells migrating through the filters were stained with DAPI followed by quantification using a Nikon Eclipse Ti Fluorescent Microscope (Nikon) and the NIS Elements software as described previously (5).

Immunofluorescence microscopy

Cells were grown on LAB-Tek II Glass Slides (Thermo Fisher Scientific) or cytospun on Shendon glass slides, then fixed with 4% formalin, permeabilized with 0.3% Triton-X (Sigma-Aldrich), and stained with phalloidin-TRITC and DNAse1-Alexa Fluor488, and DAPI. Slides were viewed using Nikon EZ-C1 Confocal Microscope (Nikon) and images processed with the NIS Elements software.

Immunoprecipitation and Western blotting

Whole-cell lysates were prepared and cleared as described previously (31). Immunoprecipitation was performed with anti-Ezrin antibody and recombinant protein A agarose beads (Thermo Fisher Scientific) then separated using NuPAGE Novex 4–12% Bis-Tris Protein Gels (Life Technologies) and transferred to polyvinylidene difluoride membranes. Protein detection was carried out using rabbit polyclonal anti-Ezrin, rabbit polyclonal anti-pERM (Cell Signaling Technology), anti-Actin, or anti-GAPDH (Abcam) antibodies. Densitometry was carried out using a GS-900 Densitometer and Image Lab Software (Bio-Rad).

Gene expression profiling

RNA was isolated using the RNeasy mini kit from L3.6pl cells with Ezrin or control shRNA following treatment with doxycycline for 72 hours. Gene expression was quantified using Illumina HT12_4 microarrays, and gene set enrichment analysis (GSEA) was performed with JAVA-based GSEA software.

Statistical analysis

Statistical differences between nonnormalized groups were analyzed using the two-tailed unpaired Student *t* test, and between normalized groups using the one-sample *t* test (GraphPad Prism Software). Statistical differences in tumor initiation frequency between groups were analyzed using the ELDA software. *P* values <0.05 were considered significant.

Results

Ezrin is overexpressed by PDAC CSCs

Ezrin is expressed in PDAC (20, 21), and we studied its expression in CSCs. Using flow cytometry, we examined PDAC cells from low-passage human xenografts derived from primary

clinical specimens and found that the $CD24^{hi}/CD44^{hi}$, $CD44^{hi}/c\text{-}Met^{hi}$, and $CD44^{hi}$ CSC populations all expressed significantly higher levels of Ezrin compared with bulk tumor cells (Fig. 1A; Supplementary Fig. S1A; refs. 3, 8, 27). Similarly, in the L3.6pl cell line Ezrin was expressed at higher levels in CSCs compared with non-CSCs (Fig. 1B). Following activation, Ezrin binds to actin (32–35), and we quantified the coprecipitation of actin with Ezrin in CSCs and differentiated PDAC cells. For these studies, we examined low-passage xenografts and enriched for CSCs by culturing as tumor spheres in serum-free media on low attachment plates and differentiated cells by exposing spheres to serum (Fig. 1C; ref. 3). We found that Ezrin activation was relatively higher in CSC-enriched tumor spheres compared with differentiated cells as evidenced by increased actin binding to Ezrin and expression of phosphorylated ERM proteins (Fig. 1D and E; Supplementary Fig. 1B). Therefore, Ezrin expression and activation are enhanced in PDAC CSCs.

Ezrin regulates CSC functions

To determine the functional role of Ezrin in PDAC, we inhibited its expression in PDAC cell lines using doxycycline-inducible shRNA constructs (Supplementary Fig. S2A). Clonogenic growth and self-renewal are hallmarks of CSCs, and we found that the inhibition of Ezrin expression for 7 days in L3.6pl cells significantly decreased subsequent tumor colony formation by >90% (Fig. 2A). Furthermore, this loss of clonogenic potential was not due to the induction of cell death or changes in proliferation (Fig. 2B; Supplementary Fig. S2B). To quantify self-renewal, we harvested and serially replated tumor colonies and found that the inhibition of clonogenic growth was maintained by L3.6pl cells containing the Ezrin shRNA vector despite the lack of doxycycline treatment during either the primary or secondary plating (Fig. 2A). Similarly, loss of Ezrin expression inhibited the formation of tumor spheres (Supplementary Fig. S2C). This loss of clonogenic growth was associated with a significant decrease in the frequency of $CD24^{+}/CD44^{+}$ (1.8% vs. 0.6 %,) and $CD44^{+}cMet^{+}$ (41% vs. 15%) CSCs (Fig. 2C). Similarly, clonogenic growth and self-renewal were significantly inhibited in E3LZ10.7 and MIA PaCa-2 cells (Supplementary Fig. S2D and S2E).

In addition to enhanced clonogenic growth, CSCs in many solid tumors have enhanced migratory capabilities that implicate a role in metastasis, and CSCs are increased in PDAC metastatic lesions (2, 5). Ezrin regulates cell migration in several malignancies (18, 19), and we found that the loss of Ezrin expression significantly inhibited the migration of L3.6pl cells by >99% (Fig. 2D) consistent with other reports (22, 23). We also carried out gain-of-function studies and overexpressed the constitutively active Ezrin-mutant T567D in L3.6pl cells and observed significantly increased colony formation (1.9-fold) and cell migration (2.2-fold) compared with cells transduced with an empty vector (Fig. 2E; Supplementary Fig. S2F). Therefore, Ezrin modulates clonogenic growth, cell migration, and the frequency of phenotypically defined PDAC CSCs.

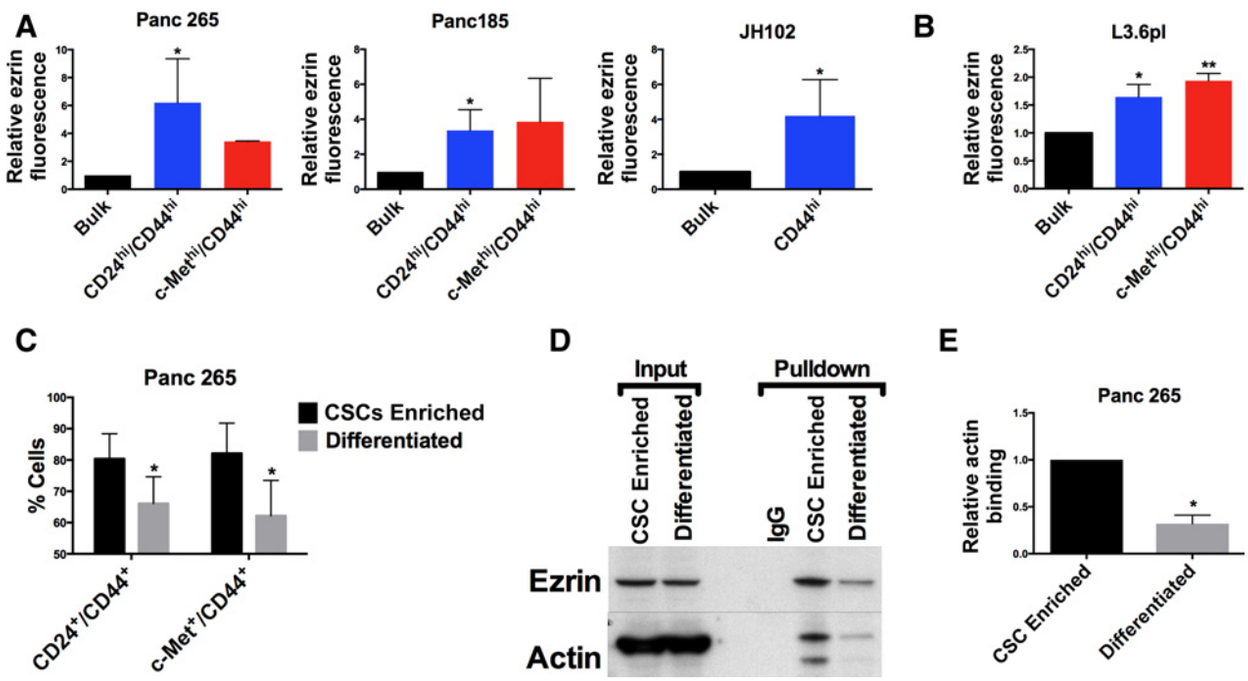

Figure 1.

Ezrin is overexpressed in PDAC CSCs. **A,** Relative mean fluorescence intensity of Ezrin expression measured by flow cytometry of Panc 265, Panc 185, and JH102 low-passage PDAC xenografts. Error bars represent SD from three independent experiments. **B,** Relative mean fluorescence intensity of Ezrin expression measured by flow cytometry of L3.6pl cells. Error bars represent SD from three independent experiments. **C,** Frequency of $CD24^{+}/CD44^{+}$ and $c\text{-}Met^{+}/CD44^{+}$ CSCs in Panc 265 cells cultured in serum-free (CSC-enriched) or serum-containing (differentiated) media. Error bars represent SD from five independent experiments. **D,** Representative Western blot analysis of actin binding to Ezrin in Panc 265 CSCs and differentiated cells as determined by coimmunoprecipitation. **E,** Quantification of relative actin binding to Ezrin by Panc 265 cells. Error bars represent SD from three independent experiments (*, $0.01<P<0.05$; **, $0.001<P<0.01$).

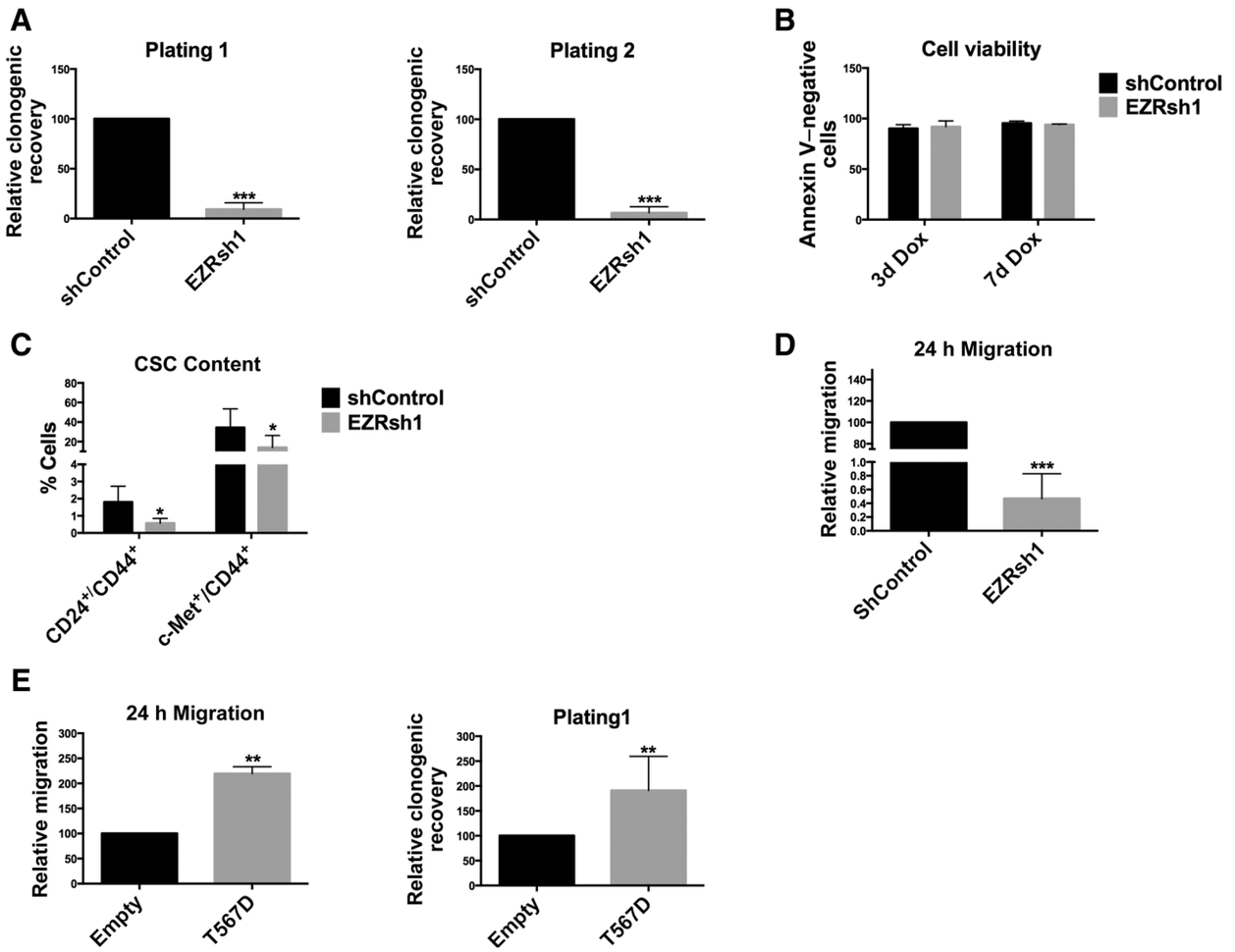

Figure 2.

Ezrin regulates CSC properties. **A,** Relative colony formation during primary and secondary plating of L3.6pl cells expressing either Ezrin shRNA or control luciferase shRNA for 7 days. Error bars represent SD from four independent experiments. **B,** Cell viability of L3.6pl cells following 3 and 7 days of Ezrin knockdown. Error bars represent SD from three independent experiments. **C,** Frequency of CSCs in L3.6pl cells after 7 days of shRNA-mediated Ezrin knockdown. Error bars represent SD from six independent experiments. **D,** Relative invasion of L3.6pl cells expressing either Ezrin or control Luciferase shRNA after 7 days of treatment with doxycycline. Error bars represent SD from four independent experiments. **E,** Relative migration and colony formation of L3.6pl cells expressing the Ezrin-mutant T567D compared with empty vector control cells. Error bars represent SD from four independent experiments (*, $0.01 < P < 0.05$; **, $0.001 < P < 0.01$; ***, $0.0001 < P < 0.001$).

Ezrin regulates actin dynamics in PDAC cells

Ezrin links the cytoplasmic tail of CD44 to F-actin leading to cytoskeletal remodeling (14), and changes in actin cytoskeletal dynamics and cell shape can direct stem cell differentiation (36–38). For example, in normal keratinocytes, self-renewal is dependent on the maintenance of a lower ratio of polymerized (F-actin) to free actin (G-actin; ref. 36). Similarly, the inhibition of actin polymerization maintains embryonic stem cells in an undifferentiated state without the need for leukemia-inhibiting factor (37). Therefore, we examined whether Ezrin regulates the actin cytoskeleton in PDAC. In L3.6pl cells, the loss of Ezrin increased cortical F-actin organization, decreased nuclear G-actin staining, and induced a flattened morphology (Fig 3A) similar to the changes seen during stem cell differentiation in normal systems (36–38). Moreover, we quantified F-actin and G-actin by flow cytometry and Western blotting analysis and observed that Ezrin knockdown significantly increased the F/G actin ratio, similar to the differentiation of epithelial stem cells (Fig. 3B; Supplementary Fig. S3A; ref. 36).

We also examined cell morphology and actin dynamics in tumor cells from low-passage PDAC xenografts and found that CSC-enriched tumor spheres were similar to control L3.6pl cells in both their morphology and actin organization (Supplementary Fig. S3B). Following serum-induced differentiation, the morphologic changes and increase in the F/G actin ratio (2.7 in CSCs vs. 4.3 in differentiated cells) were similar to L3.6pl cells following Ezrin knockdown (Supplementary Fig. S3C). We also compared $CD24^{hi}/CD44^{hi}$ CSCs and bulk tumor cells directly isolated from low-passage PDAC xenografts and found that they significantly exhibited a lower F/G actin ratio than bulk cells in two of three tumors

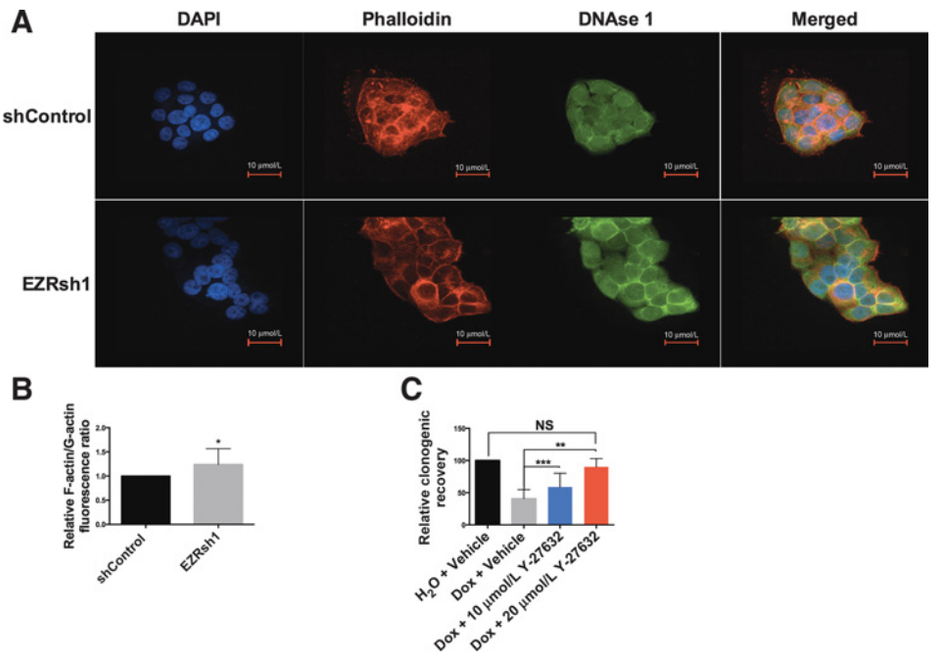

Figure 3.
Ezrin regulates actin dynamics in PDAC CSCs. **A,** F-actin (phalloidin) and G-actin (DNAse1) staining of L3.6pl cells expressing either Ezrin shRNA or control luciferase shRNA after 72 hours of doxycycline-induced knockdown (scale bar = 10 μm). **B,** Flow cytometry for F-actin (phalloidin) and G-actin (DNAse1) in L3.6pl cells after 3 days of Ezrin shRNA induction. Error bars represent SD from 10 independent experiments. **C,** Colony formation of L3.6pl cells with shRNA against Ezrin treated with Y-27632 and/or doxycycline. Y-27632 treatment was initiated 24 hours after doxycycline induction. Error bars represent SD from five independent experiments (*, $0.01 < P < 0.05$; **, $0.001 < P < 0.01$; ***, $0.0001 < P < 0.001$; NS, not significant).

(Supplementary Fig. S3D). Therefore, PDAC CSCs are associated with specific actin cytoskeletal changes that can be modulated by Ezrin.

To determine whether Ezrin maintains clonogenic growth by modulating actin dynamics, we treated L3.6pl cells with Y-27632, a small molecule that indirectly decreases actin polymerization by blocking the activity of Rho-associated kinase (ROCK; refs. 39, 40). Following Ezrin knockdown, treatment with Y-27632 significantly inhibited the loss of clonogenic growth and restored CSC-associated actin features (Fig. 3C; Supplementary Fig. S4A). In addition, we found that the inhibition of actin polymerization with Y-27632 or Cytochalasin D significantly increased the clonogenic growth of L3.6pl cells without impacting cell growth (Supplementary Fig. S4B and S4C; refs. 39, 40). In contrast, Y-27632 treatment did not impact the clonogenic recovery of L3.6pl cells expressing the constitutively active Ezrin-mutant T567D (Supplementary Fig. S4D) suggesting that the modulation of ROCK activity and subsequent inhibition of actin polymerization maintain CSCs.

ROCK can block the differentiation of mesenchymal stem cells to chondrocytes by inhibiting Sox9 expression and activity (41). Because Sox9 is also required for pancreatic development (42, 43), we studied the impact of Sox9 on Ezrin function in PDAC. We found that Ezrin knockdown resulted in a significant loss of Sox9 expression in L3.6pl cells (Supplementary Fig. S4E). However, Sox9 overexpression did not inhibit the effects of Ezrin loss on clonogenic growth (Supplementary Fig. S4F). To better understand the impact of Ezrin loss in L6.3pl cells, we carried out gene expression profiling studies and found that the loss of Ezrin expression impacted gene sets associated with the epithelial-to-mesenchymal transition and active c-Met signaling that have been associated with CSCs (Supplementary Fig. S4G; refs. 8, 44). Therefore, Ezrin maintains CSCs, at least in part, by regulating actin polymerization through ROCK inhibition, but independently of Sox9.

Pharmacologic Ezrin inhibition decreases PDAC self-renewal

We recently identified several small molecules that inhibit the phosphorylation of Ezrin at T567 and its interaction with actin (45). These compounds inhibited Ezrin-mediated invasion and survival of osteosarcoma cells *in vitro* and lung metastasis *in vivo*. We studied one of these compounds, NSC305787, in PDAC cells and found that it significantly decreased colony formation in L3.6pl (28%), E3LZ 10.7 (24%), and MIA PaCa-2 cells (57%) without inhibiting cell viability as well as inhibited the binding of Ezrin to actin (Fig. 4A; Supplementary Fig. S5). We also treated tumor spheres from low-passage PDAC xenografts with NSC305787 and found it significantly inhibited subsequent sphere formation by 17% to 40% in Panc265, Panc185, and JH102 tumors (Fig. 4B; ref. 27). Therefore, the pharmacologic inhibition of Ezrin may represent a novel strategy to target pancreatic CSCs.

Loss of Ezrin expression limits *in vivo* self-renewal

To extend our *in vitro* findings, we examined the impact of Ezrin loss on tumor initiation *in vivo*. We injected L3.6pl cells with the inducible Ezrin shRNA construct subcutaneously into immunodeficient NSG mice, and following tumor formation, administered doxycycline for 9 days (Fig. 5A; Supplementary Fig. S6A). Doxycycline treatment did not significantly impact tumor growth, although the loss of Ezrin expression resulted in histologic changes with clusters of differentiated epithelial cells as well as the inhibition of *in vitro* clonogenic growth (Fig. 5B and C; Supplementary Fig. S6B). We then collected tumors and retransplanted cells in limiting dilution into naïve recipients. In the absence of additional doxycycline treatment of the recipient mice, the tumor-initiating cell frequency during secondary engraftment of cells carrying the Ezrin shRNA construct was significantly lower than cells with the control shRNA (Table 1). Thus, transient Ezrin knockdown impairs long-term clonogenic growth and self-renewal *in vivo*.

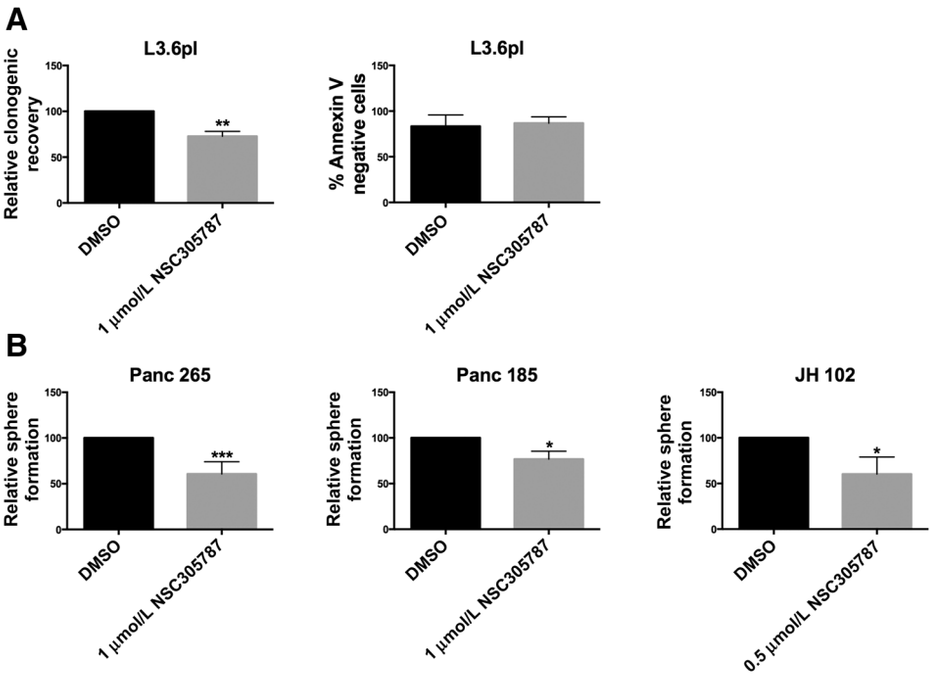

Figure 4.
Pharmacologic inhibition of Ezrin decreases PDAC self-renewal. **A,** Tumor colony formation and Annexin V surface expression of L3.6pl cells after 3 days of treatment with NSC305787. Error bars represent SD from four independent experiments. **B,** Sphere formation by low-passage human xenografts following 3 days of NSC305787 treatment. Error bars represent SD from at least four independent experiments (*, $0.01 < P < 0.05$; **, $0.001 < P < 0.01$; ***, $0.0001 < P < 0.001$).

Discussion

We found that PDAC CSCs are characterized by increased Ezrin expression and activation. The induction of Ezrin activity increases the colony-forming ability of PDAC cells, whereas the loss of Ezrin expression or activity markedly decreases migration and self-renewal *in vitro* and tumor initiation *in vivo*. We also found that a small-molecule inhibitor of Ezrin decreased the self-renewal of clinically derived PDAC samples. Therefore, Ezrin may represent a novel means of inhibiting CSCs.

We observed a decreased polymerized to free actin ratio in CSCs compared with differentiated cells, and these findings suggest that actin polymerization impacts CSC biology. In keratinocytes, the balance between free and polymerized actin can influence cell fate decisions and specific gene expression by

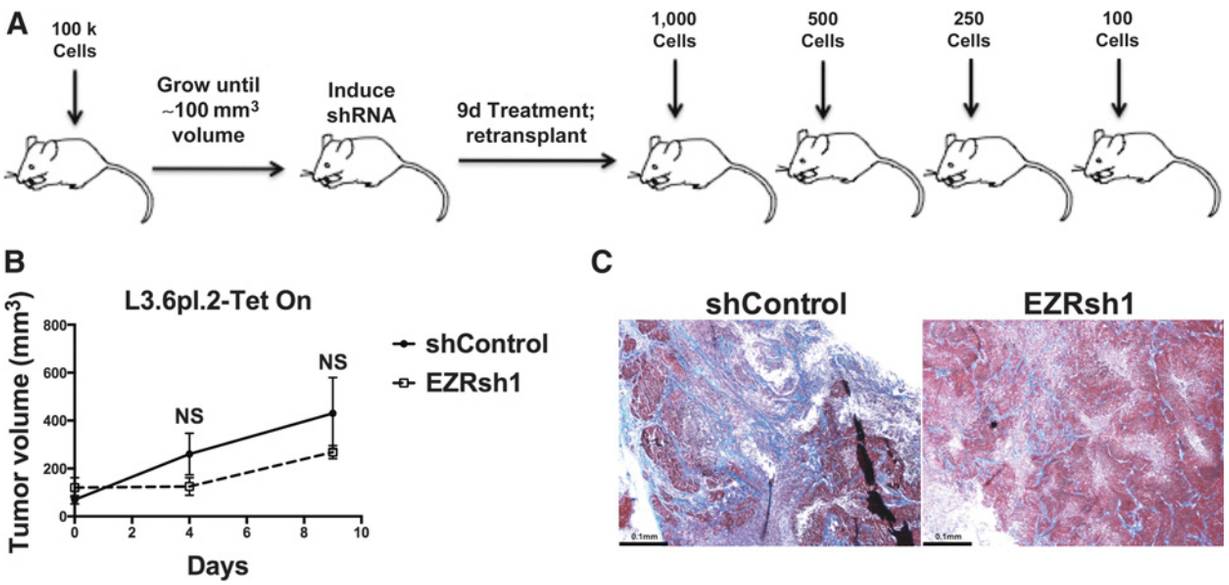

Figure 5.
Loss of Ezrin expression inhibits *in vivo* tumor-initiating potential. **A,** Experimental design. Mice with L3.6pl tumors containing control or Ezrin shRNA vectors were treated for 9 days with doxycycline. Tumors were then harvested and retransplanted in limiting dilution into naïve recipients. **B,** Mean tumor volume measured after 4 and 9 days of doxycycline treatment. Error bars represent SD ($n = 4$ mice/group). **C,** Hematoxylin and eosin staining of primary tumors from L3.6pl cells after 9 days of Ezrin shRNA induction (scale bar = 0.1 mm; NS, not significant).

Table 1. Tumor initiation in secondary recipients

	1,000 Cells	500 Cells	250 Cells	100 Cells	*P*
shControl	8/8	12/12	12/12	4/4	
EZRsh1	7/8	11/12	5/12	2/4	2.1×10^{-6}

NOTE: Extreme limiting dilution assay (ELDA) analysis of tumor initiation of tumor-derived single cells injected in secondary recipients.

regulating the availability of transcriptional cofactors (36). Although the precise mechanisms responsible for the relationship between the cytoskeleton and stem cell is unclear, it is also possible that CSCs self-renew through asymmetrical cell division, and specific cytoskeletal changes could regulate the balance between symmetric and asymmetric divisions by controlling cellular polarity (46). Alternatively, actin dynamics could serve to organize different membrane domains and modulate activity of various cell surface receptors (47, 48).

Cytoskeletal dynamics might also play a role in the interaction between tumor cells and the surrounding stroma. The deposition of extracellular matrix proteins can generate a large compressive force, and it is possible that these forces impact cytoskeletal organization leading to changes in stem cell properties. Such effects are seen during skeletal development where compressive forces lead to differentiation of progenitor cells into cartilage (49, 50). In PDAC models, the loss of stromal elements leads to disease acceleration and increased tumor-initiating cell frequency, suggesting that pressure from stroma might limit CSC self-renewal (51, 52). Thus, the maintenance of a specific actin filament organization by CSCs by restrictive pressure arising from the stroma may contribute to CSC self-renewal.

In PDAC, distinct populations of CSCs have been identified, but targeting these cells using strategies based on the expression of specific surface antigens may be limited by differential expression on some, but not all, CSCs (2). If the regulation of cytoskeletal rearrangements is necessary for the maintenance of CSCs regardless of their phenotype, then targeting actin dynamics could lead to a successful elimination of all sources of self-renewal in the tumor. Notably, we found that Ezrin was expressed in multiple, phenotypically defined CSCs. A further examination of the potential mechanisms of CSC regulation by the cytoskeleton may yield more targets for therapeutic intervention.

Small molecules that directly bind to actin and affect its polymerization have been widely used as experimental tools, including the study of normal stem cells (36, 38). However, these compounds lack specificity to a particular type of actin, and their potential effects on cardiac and skeletal muscle actin fibers limits their clinical potential (39). Thus, pharmacologic strategies to inhibit Ezrin may be a relatively safer way to modulate actin dynamics in cancer cells. We demonstrated the utility of Ezrin inhibitors in decreasing the self-renewal of PDAC cells. Because Ezrin is overexpressed in multiple tumor types, but typically not in the corresponding normal tissue of origin (15–19), it may be a promising target for pharmacologic intervention.

Disclosure of Potential Conflicts of Interest

No potential conflicts of interest were disclosed.

Authors' Contributions

Conception and design: V.R. Penchev, R. Anders, A. Maitra, A. Uren, Z. Rasheed, W. Matsui

Development of methodology: V.R. Penchev, C. Gocke, J. Li, Q. Wang, Z. Rasheed, W. Matsui

Acquisition of data (provided animals, acquired and managed patients, provided facilities, etc.): V.R. Penchev, Y.-T. Chang, A. Begum, T. Ewachiw, J. Li, R.H. McMillan, Q. Wang, R. Anders, Z. Rasheed, W. Matsui

Analysis and interpretation of data (e.g., statistical analysis, biostatistics, computational analysis): V.R. Penchev, Y.-T. Chang, T. Ewachiw, C. Gocke, R.H. McMillan, Q. Wang, R. Anders, L. Marchionni, A. Maitra, A. Uren, Z. Rasheed

Writing, review, and/or revision of the manuscript: V.R. Penchev, C. Gocke, R.H. McMillan, L. Marchionni, A. Maitra, A. Uren, Z. Rasheed, W. Matsui

Administrative, technical, or material support (i.e., reporting or organizing data, constructing databases): Y.-T. Chang, T. Ewachiw

Study supervision: Z. Rasheed, W. Matsui

Acknowledgments

The work was supported by the NIH (grant nos. R01CA150142 and R01 CA193887) to W. Matsui.

The costs of publication of this article were defrayed in part by the payment of page charges. This article must therefore be hereby marked *advertisement* in accordance with 18 U.S.C. Section 1734 solely to indicate this fact.

Received April 14, 2018; revised October 9, 2018; accepted January 8, 2019; published first January 17, 2019.

References

1. Lapidot T, Sirard C, Vormoor J, Murdoch B, Hoang T, Caceres-Cortes J, et al. A cell initiating human acute myeloid leukaemia after transplantation into SCID mice. Nature 1994;367:645–8.
2. Penchev VR, Rasheed ZA, Maitra A, Matsui W. Heterogeneity and targeting of pancreatic cancer stem cells. Clin Cancer Res 2012;18: 4277–84.
3. Li C, Heidt DG, Dalerba P, Burant CF, Zhang L, Adsay V, et al. Identification of pancreatic cancer stem cells. Cancer Res 2007;67:1030–7.
4. Hermann PC, Huber SL, Herrler T, Aicher A, Ellwart JW, Guba M, et al. Distinct populations of cancer stem cells determine tumor growth and metastatic activity in human pancreatic cancer. Cell Stem Cell 2007;1: 313–23.
5. Rasheed ZA, Yang J, Wang Q, Kowalski J, Freed I, Murter C, et al. Prognostic significance of tumorigenic cells with mesenchymal features in pancreatic adenocarcinoma. J Natl Cancer Inst 2010;102:340–51.
6. Al-Hajj M, Wicha MS, Benito-Hernandez A, Morrison SJ, Clarke MF. Prospective identification of tumorigenic breast cancer cells. Proc Natl Acad Sci U S A 2003;100:3983–8.
7. Dalerba P, Dylla SJ, Park IK, Liu R, Wang X, Cho RW, et al. Phenotypic characterization of human colorectal cancer stem cells. Proc Natl Acad Sci U S A 2007;104:10158–63.
8. Li C, JÄ Wu, Hynes M, Dosch J, Sarkar B, Welling TH, et al. c-Met Is a marker of pancreatic cancer stem cells and therapeutic target. Gastroenterology 2011;141:2218–27.
9. Tsukita S, Oishi K, Sato N, Sagara J, Kawai A, Tsukita S. ERM family members as molecular linkers between the cell surface glycoprotein CD44 and actin-based cytoskeletons. J Cell Biol 1994; 126:391–401.
10. Wakayama Y, Miura K, Sabe H, Mochizuki N. EphrinA1-EphA2 signal induces compaction and polarization of Madin-Darby canine kidney cells by inactivating Ezrin through negative regulation of RhoA. J Biol Chem 2011;286:44243–53.
11. Parisiadou L, Xie C, Cho HJ, Lin X, Gu XL, Long CX, et al. Phosphorylation of ezrin/radixin/moesin proteins by LRRK2 promotes the rearrangement of actin cytoskeleton in neuronal morphogenesis. J Neurosci 2009;29: 13971–80.

12. Manchanda N, Lyubimova A, Ho HY, James MF, Gusella JF, Ramesh N, et al. The NF2 tumor suppressor Merlin and the ERM proteins interact with N-WASP and regulate its actin polymerization function. J Biol Chem 2005; 280:12517–22.
13. Orian-Rousseau V, Chen L, Sleeman JP, Herrlich P, Ponta H. CD44 is required for two consecutive steps in HGF/c-Met signaling. Genes Dev 2002;16:3074–86.
14. Orian-Rousseau V, Morrison H, Matzke A, Kastilan T, Pace G, Herrlich P, et al. Hepatocyte growth factor-induced Ras activation requires ERM proteins linked to both CD44v6 and F-actin. Mol Biol Cell 2007;18:76–83.
15. Kang YK, Hong SW, Lee H, Kim WH. Prognostic implications of ezrin expression in human hepatocellular carcinoma. Mol Carcinog 2010;49: 798–804.
16. Elzagheid A, Korkeila E, Bendardaf R, Buhmeida A, Heikkila S, Vaheri A, et al. Intense cytoplasmic ezrin immunoreactivity predicts poor survival in colorectal cancer. Hum Pathol 2008;39:1737–43.
17. Weng WH, Ahlen J, Astrom K, Lui WO, Larsson C. Prognostic impact of immunohistochemical expression of ezrin in highly malignant soft tissue sarcomas. Clin Cancer Res 2005;11:6198–204.
18. Elliott BE, Meens JA, SenGupta SK, Louvard D, Arpin M. The membrane cytoskeletal crosslinker ezrin is required for metastasis of breast carcinoma cells. Breast Cancer Res 2005;7:R365–73.
19. Khanna C, Wan X, Bose S, Cassaday R, Olomu O, Mendoza A, et al. The membrane-cytoskeleton linker ezrin is necessary for osteosarcoma metastasis. Nat Med 2004;10:182–6.
20. Cui Y, Li T, Zhang D, Han J. Expression of Ezrin and phosphorylated Ezrin (pEzrin) in pancreatic ductal adenocarcinoma. Cancer Invest 2010;28: 242–7.
21. Oda Y, Aishima S, Morimatsu K, Hayashi A, Shindo K, Fujino M, et al. Differential ezrin and phosphorylated ezrin expression profiles between pancreatic intraepithelial neoplasia, intraductal papillary mucinous neoplasm, and invasive ductal carcinoma of the pancreas. Hum Pathol 2013; 44:1487–98.
22. Zhong ZQ, Song MM, He Y, Cheng S, Yuan HS. Knockdown of Ezrin by RNA interference reverses malignant behavior of human pancreatic cancer cells in vitro. Asian Pacific J Cancer Prev 2012;13:3781–9.
23. Meng Y, Lu Z, Yu S, Zhang Q, Ma Y, Chen J. Ezrin promotes invasion and metastasis of pancreatic cancer cells. J Translat Med 2010;8:61.
24. Bruns CJ, Harbison MT, Kuniyasu H, Eue I, Fidler IJ. In vivo selection and characterization of metastatic variants from human pancreatic adenocarcinoma by using orthotopic implantation in nude mice. Neoplasia 1999;1: 50–62.
25. Jones S, Zhang X, Parsons DW, Lin JC, Leary RJ, Angenendt P, et al. Core signaling pathways in human pancreatic cancers revealed by global genomic analyses. Science 2008;321:1801–6.
26. Meerbrey KL, Hu G, Kessler JD, Roarty K, Li MZ, Fang JE, et al. The pINDUCER lentiviral toolkit for inducible RNA interference *in vitro* and *in vivo*. Proc Natl Acad Sci U S A 2011;108:3665–70.
27. Jones S, Zhang X, Parsons DW, Lin JC, Leary RJ, Angenendt P, et al. Core signaling pathways in human pancreatic cancers revealed by global genomic analyses. Science 2008;321:1801–6.
28. Hu Y, Smyth GK. ELDA: extreme limiting dilution analysis for comparing depleted and enriched populations in stem cell and other assays. J Immunol Methods 2009;347:70–8.
29. Ishizawa K, Rasheed ZA, Karisch R, Wang Q, Kowalski J, Susky E, et al. Tumor-initiating cells are rare in many human tumors. Cell Stem Cell 2010;7:279–82.
30. Li C, Heidt DG, Dalerba P, Burant CF, Zhang L, Adsay V, et al. Identification of pancreatic cancer stem cells. Cancer Res 2007;67:1030–7.
31. Begum A, Ewachiw T, Jung C, Huang A, Norberg KJ, Marchionni L, et al. The extracellular matrix and focal adhesion kinase signaling regulate cancer stem cell function in pancreatic ductal adenocarcinoma. PLoS One 2017; 12:e0180181.
32. Turunen O, Wahlström T, Vaheri A. Ezrin has a COOH-terminal actin-binding site that is conserved in the ezrin protein family. J Cell Biol 1994; 126:1445–53.
33. Yao X, Cheng L, Forte JG. Biochemical characterization of ezrin-actin interaction. J Biol Chem 1996;271:7224–9.
34. Gungor-Ordueri NE, Tang EI, Celik-Ozenci C, Cheng CY. Ezrin is an actin binding protein that regulates sertoli cell and spermatid adhesion during spermatogenesis. Endocrinology 2014;155:3981–95.
35. Bosk S, Braunger JA, Gerke V, Steinem C. Activation of F-actin binding capacity of ezrin: synergism of PIP2 interaction and phosphorylation. Biophys J 2011;100:1708–17.
36. Connelly JT, Gautrot JE, Trappmann B, Tan DW, Donati G, Huck WT, et al. Actin and serum response factor transduce physical cues from the microenvironment to regulate epidermal stem cell fate decisions. Nat Cell Biol 2010;12:711–8.
37. Murray P, Prewitz M, Hopp I, Wells N, Zhang H, Cooper A, et al. The self-renewal of mouse embryonic stem cells is regulated by cell-substratum adhesion and cell spreading. Int J Biochem Cell Biol 2013;45:2698–705.
38. McBeath R, Pirone DM, Nelson CM, Bhadriraju K, Chen CS. Cell shape, cytoskeletal tension, and RhoA regulate stem cell lineage commitment. Dev Cell 2004;6:483–95.
39. Bonello TT, Stehn JR, Gunning PW. New approaches to targeting the actin c ytoskeleton for chemotherapy. Future Med Chem 2009;1:1311–31.
40. Maekawa M, Ishizaki T, Boku S, Watanabe N, Fujita A, Iwamatsu A, et al. Signaling from Rho to the actin cytoskeleton through protein kinases ROCK and LIM-kinase. Science 1999;285:895–8.
41. Woods A, Wang G, Beier F. RhoA/ROCK signaling regulates Sox9 expression and actin organization during chondrogenesis. J Biol Chem 2005;280: 11626–34.
42. Matsumoto Y, Inden M, Tamura A, Hatano R, Tsukita S, Asano S. Ezrin mediates neuritogenesis via down-regulation of RhoA activity in cultured cortical neurons. PLoS One 2014;9:e105435.
43. Seymour PA, Freude KK, Tran MN, Mayes EE, Jensen J, Kist R, et al. SOX9 is required for maintenance of the pancreatic progenitor cell pool. Proc Natl Acad Sci U S A 2007;104:1865–70.
44. Mani S, Evans K, Hollier B, Guo W, Weinberg R. Generation of stem-like cells via EMT: a new twist in cancer initiation and progression. Am Assoc Cancer Res Educ Book 2009;173–8.
45. Bulut G, Hong SH, Chen K, Beauchamp EM, Rahim S, Kosturko GW, et al. Small molecule inhibitors of ezrin inhibit the invasive phenotype of osteosarcoma cells. Oncogene 2012;31:269–81.
46. Dard N, Louvet-Vallee S, Santa-Maria A, Maro B. Phosphorylation of ezrin on threonine T567 plays a crucial role during compaction in the mouse early embryo. Dev Biol 2004;271:87–97.
47. Donatello S, Babina IS, Hazelwood LD, Hill AD, Nabi IR, Hopkins AM. Lipid raft association restricts CD44-ezrin interaction and promotion of breast cancer cell migration. Am J Pathol 2012;181:2172–87.
48. Yakovich AJ, Huang Q, Du J, Jiang B, Barnard JA. Vectorial TGFbeta signaling in polarized intestinal epithelial cells. J Cell Physiol 2010;224: 398–404.
49. Rooney P, Archer CW. The development of the perichondrium in the avian ulna. J Anat 1992;181:393–401.
50. Long F, Linsenmayer TF. Regulation of growth region cartilage proliferation and differentiation by perichondrium. Development 1998;125: 1067–73.
51. Ozdemir BC, Pentcheva-Hoang T, Carstens JL, Zheng X, Wu CC, Simpson TR, et al. Depletion of carcinoma-associated fibroblasts and fibrosis induces immunosuppression and accelerates pancreas cancer with reduced survival. Cancer Cell 2014;25:719–34.
52. Rhim AD, Oberstein PE, Thomas DH, Mirek ET, Palermo CF, Sastra SA, et al. Stromal elements act to restrain, rather than support, pancreatic ductal adenocarcinoma. Cancer Cell 2014;25:735–47.